Change in Inertial Confinement Fusion Implosions upon Using an *Ab Initio* Multiphase DT Equation of State

L. Caillabet, B. Canaud,* G. Salin, S. Mazevet, and P. Loubeyre

CEA, DAM, DIF, F-91297 Arpajon, France

(Received 17 May 2011; published 8 September 2011)

Improving the description of the equation of state (EOS) of deuterium-tritium (DT) has recently been shown to change significantly the gain of an inertial confinement fusion target [S. X. Hu *et al.*, Phys. Rev. Lett. **104**, 235003 (2010)]. Here we use an advanced multiphase EOS, based on *ab initio* calculations, to perform a full optimization of the laser pulse shape with hydrodynamic simulations starting from 19 K in DT ice. The thermonuclear gain is shown to be a robust estimate over possible uncertainties of the EOS. Two different target designs are discussed, for shock ignition and self-ignition. In the first case, the areal density and thermonuclear energy can be recovered by slightly increasing the laser energy. In the second case, a lower in-flight adiabat is needed, leading to a significant delay (3 ns) in the shock timing of the implosion.

DOI: 10.1103/PhysRevLett.107.115004 PACS numbers: 52.25.Kn, 52.57.−z, 52.65.Pp, 62.50.−p

The deuterium-tritium (DT) equation of state (EOS), starting from the cryogenic solid and undergoing a wide range of plasma conditions, is a key input to simulate the inertial confinement fusion (ICF) implosion of the DT pellet and hence to quantify the fusion energy production. The current uncertainty in the EOS of DT, more particularly in the strongly correlated and degenerate regime, is maintaining uncertainties in hydrosimulations for the prediction of ICF thermonuclear gains and also for the shock timing design. Recently, Hu *et al.* [1] have shown a significant reduction (30%) of the thermonuclear gain by improving the DT EOS in the strongly coupled and degenerate regime. A direct implication of this work is the reduction of the safety margin in current ICF designs that could be deleterious to achieve high gains. But, no reoptimization of the laser pulse has been performed with this partial *ab initio* EOS, only valid for $T \geq 1.35$ eV. Consequently, that poses two important questions: can the decrease in thermonuclear energy be avoided by reshaping the laser pulse, and what result would this have on the tuning of shock timing? The aim of the present work is to address these two questions.

Here we use a recently published multiphase DT EOS [2], dubbed MP EOS, that is based on *ab initio* calculations in the strongly coupled and degenerate regime ($\rho = 0.5$–12.5 g/cc and $T \leq 10$ eV), and extended here to cover the whole thermodynamical path of DT ice ($\rho = 0.25$–4×10^3 g/cc and $T = 0$–10 keV). Hydrosimulations can thus start at the realistic temperature of 19 K for DT ice, that allows us to take into account the effect of the solid-liquid transition and to avoid any effect of preheating of the shell. Two different target designs are considered, one for shock ignition and the other for self-ignition, corresponding to two different thermodynamic paths for the compression of the DT fuel. It will be shown below that the energy gain of the target is in fact a robust estimate that can be recovered after optimization of the laser pulse. But the use of a more realistic EOS can lead to large changes in the shock timing.

In classical inertial confinement fusion [3,4], a single shell of cryogenic DT ice, enclosing the DT gas, is accelerated inward by laser irradiation in direct-drive (DD) [5] or by x rays in indirect drive [6]. A shaped laser pulse creates a multiple-shock train that travels through the target towards the center. To achieve a net energy gain, a very high-density DT shell should be assembled by an in-flight compression around the very hot DT gas. Two quantities are more specifically varied to control the characteristic of the implosion: the pressure after the first shock that sets the value of the in-flight adiabat of the compression path (defined as the ratio of the multiple-shock induced-pressure over the Fermi pressure, $\alpha = P\,[\mathrm{GPa}]/217\rho^{5/3}\,[\mathrm{g/cc}]$), and the peak implosion velocity of the DT ice shell that scales with the internal energy given to the DT fuel. During the implosion, the central gas and the cryogenic DT shell follow two very different thermodynamic paths. The gas stays in a hot, weakly coupled and classical regime (the coupling parameter $\Gamma = e^2/a_i k_B T \ll 1$, where a_i is the ionic sphere radius, and the degeneracy parameter $\theta = T/T_F \gg 1$ with T_F the Fermi temperature of the electron gas). This regime is well described by physical models [7–12]. The SESAME EOS [7], based on physical models, gives a good description of the compression of the DT gas during the implosion and is used in the present work. On the other hand, the compression of DT ice goes through strongly coupled and degenerate plasma states, certainly throughout the deposition time of the laser energy to the pellet when the multishocks cross the target. In this case, many-body effects on the EOS are important and can only accurately be described by *ab initio* methods: quantum molecular dynamic (QMD) for low temperatures and path integral Monte Carlo (PIMC) calculations for high temperatures. The MP EOS

[2] is at present the most advanced EOS of DT to treat the states of strong coupling and degeneracy. The MP EOS, applied to DT, covers the range 0.5–12 g/cc, and up to $T = 10$ eV, and synthesizes the QMD [13–15] and PIMC calculations [1,16] published so far in this domain. In addition, this EOS takes into account the quantum contributions of the nuclei. It has been shown to successfully reproduce all of the experimental data on the EOS of H_2 and D_2 published in the solid, the molecular fluid, and the plasma state. We have extended it by performing *ab initio* calculations down to $\rho = 0.25$ g/cc in the same range of temperatures, in order to have an *ab initio* description of the cryogenic DT at the initial condition of 19 K. The MP EOS converges to the model of Chabrier and Potekhin [11,12] in the limits of the domain of *ab initio* calculations, and this model is then used to extend the MP EOS over the thermodynamical range of the compression of the DT ice shell, i.e., up to densities of 10^3 g/cc and temperatures of 10 keV. The intermediate domain in density between the gas and the solid is never traversed at low or warm temperature during the implosion, so an accurate description of this domain is not necessary here. For a given pressure and temperature, discrepancies in the energy and in the pressure between the MP EOS and the SESAME EOS are $\geq 5\%$ when $T \leq 86$ eV in the density range 0.25–25 g/cc. This is illustrated in Fig. 1 by comparing the principal Hugoniot curves derived from the MP EOS and the SESAME EOS, that shows a clear difference in compressibility of the DT ice under dynamic loading. The implication of such differences in the DT EOS for the optimization of ICF implosion is discussed below for two ICF targets, the Laser Megajoule (LMJ) baseline direct-drive design [17] and a shock-ignited HiPER-like direct-drive design [18]. Hydrodynamic calculations were performed with the multidimensional Lagrangian radiation-hydrodynamics code FCI2 [19] employed here in its one-dimensional version. It includes inverse-bremsstrahlung laser absorption with a one-dimensional ray-tracing package, flux-limited Spitzer heat conduction, multigroup radiative transfer, and multigroup fusion-product transport. Both designs are directly driven by shaped UV-laser pulses.

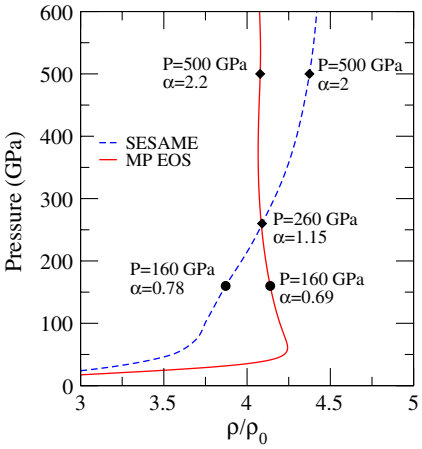

FIG. 1 (color online). Principal Hugoniot curve of the cryogenic DT ($\rho_0 = 0.25$ g/cc, $T_0 = 19$ K) for the MP EOS and SESAME EOS [7]. The diamonds (circles) indicate the pressure and the in-flight adiabat behind the first shock induced by the laser pulse in the LMJ target (HiPER-like target).

The HiPER-like target consists of a 316 μm-thick "all-DT" spherical pellet with a 1244 μm inner radius [18]. The results of four hydrosimulations are presented in Fig. 2. First, an optimization of the laser pulse shape is done using the SESAME EOS, with a pressure after the first shock of 160 GPa corresponding to an in-flight adiabat of $\alpha = 0.78$ and a peak velocity of 290 km/s. Second, the MP EOS is used, keeping the same laser pulse. Third, the laser pulse is redesigned using the MP EOS and keeping the implosion velocity at 290 km/s. Finally, the drive part of the laser pulse is increased in order to recover the same thermonuclear energy as that in the first case but with the MP EOS. By replacing the SESAME EOS by the MP EOS and keeping the laser pulse optimized with the SESAME EOS, significant differences appear at the beginning of the implosion that act on the in-flight adiabat and on the implosion velocity. This results in a large reduction of the peak areal density at stagnation as well as in the thermonuclear energy (of about 7% and 60%, respectively). The decrease of the thermonuclear energy

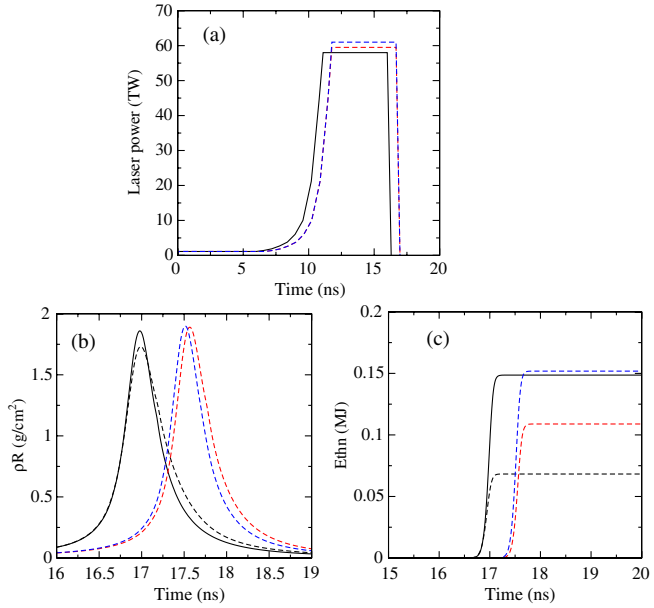

FIG. 2 (color online). Output of the hydrodynamic simulations of the HiPER-like target. (a) The laser pulse, (b) the areal density, and (c) the thermonuclear energy as a function of time. The solid lines represent hydrodynamic simulations with the SESAME EOS; the dashed lines represent hydrodynamic simulations where the SESAME EOS has been replaced by the MP EOS, keeping the initial laser pulse (black dashed line), the initial implosion velocity [light gray (red) dashed line], and the initial thermonuclear energy [dark gray (blue) dashed line].

qualitatively confirms the less efficient compression of the DT fuel when strong correlation and degeneracy effects in the plasma are accurately taken into account, as pointed out by Hu *et al.* [1]. This is related to the significant modification of the thermodynamic path followed by the DT shell during implosion. In particular, the density and temperature at stagnation are significantly modified (the average density and temperature of the shell at stagnation are 319 g/cc and 0.63 keV with the SESAME EOS and 285 g/cc and 0.53 keV with the MP EOS).

As the implosion history is connected to shock propagation, an accurate shock timing analysis is needed. The foot of the laser pulse creates a first shock at a pressure of 160 GPa which corresponds to a 6.6% higher density when using the MP EOS instead of the SESAME EOS (see Fig. 1). Consequently, the secondary shock propagates faster in the already compressed shell of DT and catches up to the first shock created by the foot. This leads to a shock mistiming which can easily be corrected by delaying the main drive of the laser pulse in time. Indeed, in order to maximize the peak areal density, the main peak of the laser pulse has to be delayed by 670 ps. With this optimized shock timing, a slight decrease (1%) in the peak implosion velocity v_{imp} is still observed. Since the peak kinetic energy is completely transformed into internal energy during deceleration, this leads to a reduced thermonuclear energy. The same implosion velocity can be recovered by slightly increasing the main drive power (from 357 to 364 kJ). With the revised laser pulse shown in Fig. 2(a), the value of the areal density is recovered with the SESAME EOS but a significant reduction of the thermonuclear energy of about 27% is still observed [see Figs. 2(b) and 2(c)]. To recover the thermonuclear energy, the laser energy has to be further increased to 374 kJ. For all these cases, the solid-liquid phase transition appears to have no effect. This is confirmed by simulations started at a higher temperature (30 K) than the triple point temperature which give the same results. In conclusion, using the more realistic MP EOS, the shock timing of the laser pulse has to be modified by 670 ps and the energy of the laser increased by 5% in order to recover the performance of the target calculated using the SESAME EOS.

The direct-drive baseline design for the LMJ target is a massive 1642 μm outer radius, 1 μm-thick CH layer, 202 μm-thick wetted foam and 164 μm-thick DT ice inner-layer capsule [17]. Four hydrosimulations output are performed and presented in Fig. 3. As previously, the first one concerns the optimization done with SESAME EOS. The pressure after the first shock is 500 GPa, which corresponds to an in-flight adiabat of $\alpha = 2$. The peak implosion velocity is 400 km/s, and a thermonuclear energy of 82 MJ is obtained for a 1D-incident laser energy of 1 MJ. The second case concerns the implosion done with the same laser pulse shape and the MP EOS instead of the SESAME EOS. As for both the HiPER-like target discussed above and

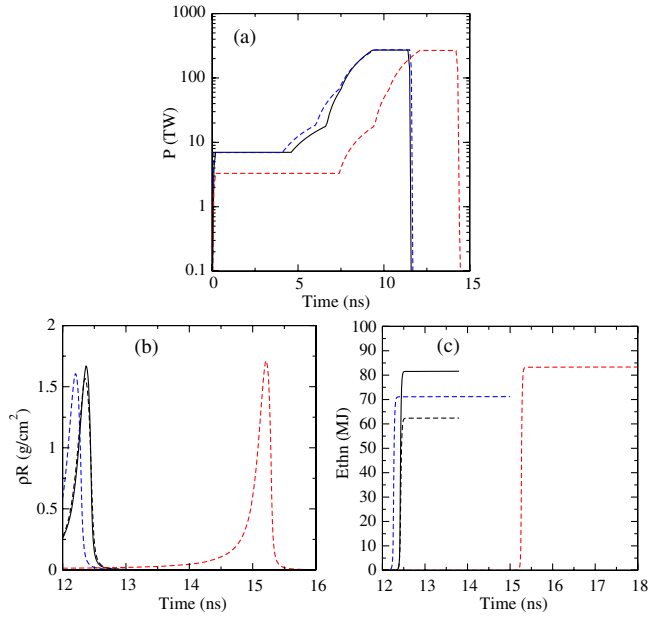

FIG. 3 (color online). Output of the hydrodynamic simulations of the LMJ baseline DD target. (a) The laser pulse, (b) the areal density, and (c) the thermonuclear energy as a function of time. The solid lines represent hydrodynamic simulations optimized with the SESAME EOS at a first shock pressure of 500 GPa; the black dashed lines represent hydrodynamic simulations where the SESAME EOS has been replaced by the MP EOS, keeping the initial laser pulse; the dark gray (blue) dashed lines represent hydrodynamic simulations optimized with the MP EOS at a first shock pressure of 500 GPa; the light gray (red) dashed lines represent hydrodynamic simulations optimized with the MP EOS at a first shock pressure of 260 GPa.

Hu's work, a reduction ($\sim 7\%$) of the areal density and a significant decrease ($\sim 30\%$) of the output thermonuclear energy are observed. The third case concerns the optimization of the laser pulse using the MP EOS and keeping the peak implosion velocity at 400 km/s. The laser ramp is modified as shown in Fig. 3 and an optimum is achieved with a thermonuclear energy of 71 MJ. The peak areal density occurs 200 ps earlier than in the first case mainly due to the higher compressibility of the SESAME EOS compared to the MP EOS at 500 GPa. Increasing the peak implosion velocity increases the thermonuclear energy to a maximum of 77 MJ, which is still 6% below the SESAME result. In fact, the MP EOS produces much more entropy along a compression path than the SESAME EOS. The only way to counterbalance this increase consists in choosing a lower in-flight adiabat. This is performed in a fourth case by tuning the post-first-shock pressure to 260 GPa (crossing point of the Hugoniot curves of the SESAME and the MP EOS, as shown in Fig. 1) and leads to a lower in-flight adiabat of 1.15 instead of 2.2. The laser pulse shape is then optimized to obtain the same implosion velocity of 400 km/s. The calculation produces a 1D-thermonuclear energy of 82 MJ for a laser pulse energy of 971 kJ, hence recovering the previous value obtained with the SESAME

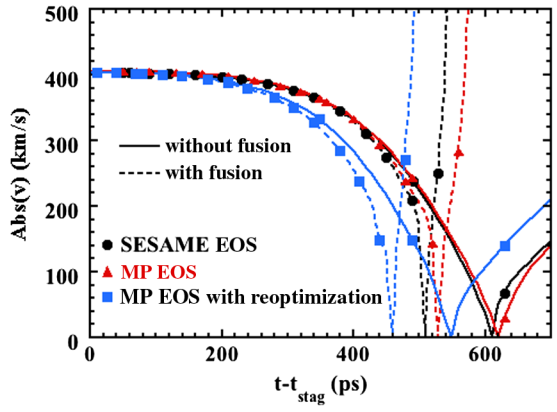

FIG. 4 (color online). Deceleration of the LMJ baseline DD target with and without nuclear reactions.

EOS. But in that case a strong difference in the shock timing is observed. The peak areal density is delayed by 3 ns. In addition, a lower in-flight adiabat could deteriorate the hydrodynamic stability of the implosion. However, that is beyond the scope of the present work.

Looking at the deceleration phase illustrates the difference between both EOS and their impact on the conversion of the peak kinetic energy into internal energy of the fuel. When the laser ends, the kinetic energy reaches a maximum and the deceleration phase begins. During this stage, the kinetic energy is converted in internal energy of the hot spot and the shell, and this transfer is strongly coupled to the EOS. The comparison of the implosion velocity versus time (cf. Fig. 4) from its maximum value to stagnation in two cases, either when thermonuclear fusion reactions are turned on or off, allows us to estimate the kinetic energy of the DT shell in excess when ignition occurs.

Stagnation occurs earlier with thermonuclear reactions than without as shown in Fig. 3. The kinetic energy margin is defined as the ratio of the kinetic energy of the DT shell without fusion at the time of stagnation of the implosion with fusion over the peak kinetic energy. As seen in Fig. 3, the SESAME case leads to a kinetic margin of 27% and the MP EOS case of 21% before optimization. After reoptimization, the margin grows to 24%. With the same kinetic energy, The SESAME EOS is more efficient than the MP EOS to convert kinetic energy into ionic temperature (T_i) and areal density (ρR) at stagnation. The ignition thermodynamic conditions ($T_i > 6$ keV and $\rho R > 0.2$ g/cm^2) are met latter with the MP EOS than with the SESAME EOS. This indicates a greater entropy change during the compression with the MP EOS.

In conclusion, we have shown the change in the implosion characteristics for two ICF targets, using an improved treatment for the effect of strong coupling and degeneracy in the equation of state of DT. A newly developed MP EOS was used to perform a full optimization of the ICF implosion under a given laser energy, starting from the cryogenic conditions of 19 K. For a given density or temperature condition, the MP EOS has a higher entropy than the SESAME EOS commonly used. If the in-flight adiabat is low enough, slightly more energy than is predicted with the SESAME EOS will be needed to reach a given thermonuclear yield. However, if the first shock is too high, the thermonuclear yield cannot be recovered, even with a large increase in the laser input energy. In this case, the first shock pressure has to be reduced, recovering the thermonuclear yield without changing the input energy. Consequently, the present work demonstrates that the uncertainty in the DT EOS will not jeopardize predictions for ICF ignition. The use of a more advanced EOS such as the MP EOS is expected to be a valuable way to scale ICF compression with improved predictions for the shock timing which, as shown here, may change by up to 3 ns.

*Corresponding author.
benoit.canaud@cea.fr

[1] S. X. Hu, B. Militzer, V. N. Goncharov, and S. Skupsky, Phys. Rev. Lett. **104**, 235003 (2010).
[2] L. Caillabet, S. Mazevet, and P. Loubeyre, Phys. Rev. B **83**, 094101 (2011).
[3] J. Nuckolls, L. Wood, A. Thiessen, and G. Zimmerman, Nature (London) **239**, 139 (1972).
[4] S. Atzeni and J. Meyer-Ter-Vehn, *The Physics of Inertial Fusion* (Clarendon, Oxford, 2004).
[5] B. Canaud, F. Garaude, C. Clique, N. Lecler, A. Masson, R. Quach, and J. Van der Vliet, Nucl. Fusion **47**, 1652 (2007).
[6] J. Giorla *et al.*, Plasma Phys. Controlled Fusion **48**, B75 (2006).
[7] E. S. Hertel, G. I. Kerley, Sandia National Laboratories Technical Report No. SAND98-0945-0947, 1998; G. I. Kerley, Phys. Earth Planet. Inter. **6**, 78 (1972).
[8] D. Saumon *et al.*, Astrophys. J. Suppl. Ser. **99**, 713 (1995).
[9] M. Ross, Phys. Rev. B **58**, 669 (1998).
[10] H. Juranek and R. Redmer, J. Chem. Phys. **112**, 3780 (2000).
[11] G. Chabrier and A. Y. Potekhin, Phys. Rev. E **58**, 4941 (1998).
[12] A. Potekhin and G. Chabrier, Contrib. Plasma Phys. **50**, 82 (2010).
[13] T. J. Lenosky, S. R. Bickham, J. D. Kress, and L. A. Collins, Phys. Rev. B **61**, 1 (2000).
[14] B. Holst, N. Nettelmann, and R. Redmer, Contrib. Plasma Phys. **47**, 368 (2007).
[15] M. A. Morales, C. Pierleoni, and D. M. Ceperley, Phys. Rev. E **81**, 021202 (2010).
[16] B. Militzer and D. M. Ceperley, Phys. Rev. Lett. **85**, 1890 (2000).
[17] B. Canaud, X. Fortin, F. Garaude, C. Meyer, F. Philippe, M. Temporal, S. Atzeni, and A. Schiavi, Nucl. Fusion **44**, 1118 (2004).
[18] B. Canaud and M. Temporal, New J. Phys. **12**, 043037 (2010).
[19] E. Buresi, J. Coutant, and R. Dautray, Laser Part. Beams **4**, 531 (1986).